Proceedings of FEDSM2006
2006 ASME Joint U.S. - European Fluids Engineering Summer Meeting
July 17-20, Miami, FL

FEDSM2006-98459

Representing Polydispersed Droplet Behavior in Nucleating Steam Flow with the Quadrature - Method - of - Moments

A. Mousavi
Dept. of Mechanical Engineering, University of New Brunswick, Fredericton, Canada, e-mail : arash.mousavi@unb.ca

A.G. Gerber
Dept. of Mechanical Engineering, University of New Brunswick, Fredericton, Canada, e-mail : agerber@unb.ca

M.J. Kermani
Dept. of Mechanical Engineering, Amir Kabir University of Technology (Tehran Polytechnic), Iran, e-mail : mkermani@aut.ac.ir

Abstract

This paper applies the Quadrature-Method-of-Moments (QMOM) to the polydispersed droplets spectrums typical in low pressure steam turbines. Various modes of nonequilibrium phase transition are present in steam turbines, starting with primary and secondary homogeneous nucleation as the main source of moisture followed by heterogeneous nucleation and surface entrainment sources. The range of phase transition possibilities leads to a wide range of droplet sizes, which are present under various combinations of inertial and thermal nonequilibrium. Given the extensive prevalence of CFD in turbomachinery design, it is of interest to develop an efficient modeling approach for polydispersed droplet flows that avoids solving an excessive number of equations to represent the droplet size distribution. Methods based on QMOM have shown promise in this regard in other applications areas of two-phase flow, and this paper attempts to quantify its potential for steam turbine applications by applying the method to supersonic nozzle studies with homogeneous and heterogeneous phase transitions.

1. Introduction

Steam turbines are widely used in power plants and their efficient operation is important to the economic success of any plant. Formation of water droplets by various phase transition mechanisms in the low pressure stages of the turbine is often mentioned as an important source of power loss and blade erosion problems. Due to the complex transonic flow conditions present, the formation of these droplets occurs under highly non-equilibrium conditions with increased irreversible losses present.

For this reason steam turbine operation research has focused increasingly on the handling of moisture formed in the low pressure stages. Beside extensive experimental efforts on nonequilibrium phase transition, research into Computational-Fluid-Dynamics (CFD) models of increasing complexity to investigate phase transition phenomena has also been on-going [1-8]. The formation of wetness, and its subsequent transport, under practical turbine operating conditions, results in a wide range of droplets sizes which pose a significant challenge for efficient and accurate modeling. Furthermore the droplets exist under varying degrees (and combinations) of thermal and inertial nonequilibrium. Presently most of the models for phase transition in steam turbines assume monodispersed size distributions [1-8] at any point in the flow, which can lead to considerable errors when predicting machine efficiency and/or the behavior and distribution of droplets for erosion control. The focus of the present work is on the application of a new method, based on the Method-of-Moments (MOM) [9], for representing polydispersed droplet conditions present in a steam turbine. The droplets studied in this work are a result of condensation through heterogeneous and homogeneous nucleation in size ranges typical for steam turbines.

The method investigated in this paper is a variant of the MOM methodology, termed the Quadrature Method of Moments (QMOM) [10] and is similarly based on tracking the lower order moments of a droplet (in this case size) distribution. The lower order moments are obtained in the CFD solution through solving moment transport equations with appropriate contributing source terms. In the QMOM methodology the lower order moments, unlike in MOM, are used to obtain a representative discrete distribution of the droplet sizes and their weights. The obtained sizes and weights can be applied to the moment transport equations to close integrals of the number density function. A previous study [11] on the application of QMOM to conditions relevant to steam turbine flows has shown its potential for representing a wide range of droplet sizes with a single set of moment equations. The MOM approach has been applied to nucleating steam flows but is unable to handle the growth

equations in condensing steam without approximation [12]. In this regard QMOM shows promising behavior as any kind of growth law can be applied. The present study considers the QMOM methodology, fully coupled to the hydrodynamic solutions in a supersonic nozzle along with heterogeneous and homogeneous droplet nucleation active. The evolution of the polydispersed size distribution and its statistics are examined in light of the QMOM method.

2. Governing Equations

In the present study we consider 1-D supersonic flow conditions in order to isolate our study of the QMOM method. Furthermore, the study considers two modes of nucleation as active in the flow. The first is heterogeneous nucleation on foreign nuclei in the size range of 0.01 to 1 μm, and the second homogeneous nucleation, introducing droplets initially in the range of 0.001 and after growth 0.01 to 0.1 μm. Since the droplets in this study remain nominally below 1 μm in size the effect of slip can be neglected. The transport equations for mass and momentum can then be formulated in terms of mixture properties with additional transport equations to represent the droplet distribution. Significant thermal nonequilibrium conditions develop in the flow requiring a transport equation for mixture energy. Associated thermodynamic irreversibilities are incorporated through a heat transfer model in the droplet growth calculation. Details on the various formulations now follow.

2.1. Gas (continuous) phase

The governing equations of fluid motion for quasi one-dimensional, compressible flow of a two-phase mixture in full conservative form with no body force can be written as [14]:

$$\frac{\partial(SQ)}{\partial t}+\frac{\partial F}{\partial x}-H_s=0 \tag{1}$$

where t is time, x is a space coordinate and S is the cross sectional area of the duct. Furthermore Q, F and H_s are respectively the conservative vector, flux vector and source term responsible for the area change, given below:

$$Q=\begin{bmatrix}\rho\\ \rho u\\ \rho e_t\end{bmatrix}, F=S\begin{bmatrix}\rho u\\ \rho u^2+p\\ \rho u H\end{bmatrix}, H_s=\frac{\partial S}{\partial x}\begin{bmatrix}0\\ p\\ 0\end{bmatrix} \tag{2}$$

Here ρ is the two-phase mixture density, u is the velocity, e_t, the total mixture internal energy, p the pressure and H the total mixture enthalpy. Due to the small size of the droplets considered, the temperature of the condensed phase can be determined as a function of its size and will be elaborated on subsequently.

2.2. Liquid (dispersed) phase

The liquid phase influences the governing transport equations for mass, momentum and energy through the wetness (or mass fraction) level. Determination of the condensed phase wetness and diameter distribution in the flow is based on the moment transport equations solved in conjunction with the QMOM method. The appearance of the condensed phase in the flow depends on the nucleation models, and the developed meta-stable conditions in the flow. The growth of released droplets in the flow field depends on droplet growth models which embody the local heat transfer conditions that drive heat and mass transfer in supercooled vapor conditions. The discussion of the interaction of these models begins with a description of the method of moments for representing size distributions.

2.2.1. Moment transport equation. The method of moments (MOM), as applied in our tests, is based on using lower-order moments to represent the droplet size distribution, with the advantage that no additional information of the distribution function is required. The moments evolve in response to particle growth and nucleation, and are used to close any integrals of the droplet density function (f) that may appear in transport equations. The development of the MOM equations and its relation to the number density equation has been described in a previous paper [11], and only the highlights are presented here. Considering only one internal coordinate (the droplet radius) the number density transport equation, including the change in internal coordinate (G) (the growth law), change in external coordinate (u_i) and nucleation (h), is shown below

$$\frac{\partial \rho f}{\partial t}+\sum_{i=1}^{3}\frac{\partial(u_i\rho f)}{\partial x_i}+\frac{\partial(G\rho f)}{\partial r}=\rho h \tag{3}$$

where u_i is local velocity and h has the units number of particles introduced into the system per unit of mixture mass at time t. Both the growth law and nucleation function depend on droplet radius and are considered as known. This enables Eq.3 to be solved together with the mass, momentum and energy equations for the two phase system. The main problem in dealing with Eq.3 is the unknown distribution function f. To handle this problem, f is represented through its lower order moments. With the internal dimensions reduced to the droplet radius r, the moments of f are as following:

$$\mu_k=\int r^k f dr\,, k=0,1,2,... \tag{4}$$

This allows Eq. 3 to be represented instead through transport equations of its moments now written as:

$$\frac{\partial \rho\mu_k}{\partial t}+\sum_{i=1}^{3}\frac{\partial(u_i\rho\mu_k)}{\partial x_i}-k\int r^{k-1}\rho G f dr=\rho J r_{crit}^k$$
$$k=0,1,2,... \tag{5}$$

where J is nucleation rate per unit mass of mixture. Nucleation occurs only at certain critical radii depending on the nucleation model, so that h and J are related through a Dirac delta function as:

$$h=J\delta(r-r_{crit}) \tag{6}$$

The solution of Eq.5 involves integrals of the number density function and therefore is limited to a specific form of growth law where:

$$G(r)=a_1+a_2 r \tag{7}$$

This is the form of equation used in the MOM with any other form having to be approximated using various means [12]. To handle this limitation, McGraw [10] developed QMOM that involves replacing the integral in Eq.5 by a summation of weights (w_i) and abscissas (r_i) which are obtained as a result of a Gaussian quadrature procedure. The integral would then be written in the form:

$$k\int r^{k-1}G(r)\,f dr \cong k\sum_{i=1}^{n} r_i^{k-1}G(r_i)w_i\,,\; k \geq 1 \tag{8}$$

It should be noted that abscissas and weights are independent of particle growth law G and distribution function f. The moments are written in the new form of

$$\mu_k = \int r^k n(r)dr = \sum_{i=1}^{n} r_i^k w_i \tag{9}$$

Finally for 1-D flow the moment transport equations, originally presented in Eq.5, now becomes:

$$\frac{\partial \rho\mu_k}{\partial t} + \frac{\partial\left(u\rho\mu_k\right)}{\partial x} - \rho k\sum_{i=1}^{n} r_i^{k-1}G(r_i)w_i = \rho J r_{crit}^k$$
$$k = 0,1,2,...,2n-1 \tag{10}$$

The number of moments is $2n$, the optimum value of n is based on accuracy and efficiency considerations, and is recommended by Marchisio [15] to be three. This is the value of n chosen in this work. With the moments of the distribution available the weights, w_i, and sizes, r_i, are obtained by applying a product difference algorithm as described in [10].

2.2.2. Droplet nucleation and growth. Appearance of the liquid phase occurs through the process of homogeneous and heterogeneous nucleation, which in either case occurs when free energy barriers to the formation of small spherical droplets are overcome. In the case of heterogeneous nucleation foreign nuclei are present which reduces the barriers, and phase transition can occur at lower levels of critical supercooling. In the case of homogeneous nucleation the phase transition occurs spontaneously out of the vapor phase, and generally requires significantly more supercooling than the heterogeneous case. The nucleated droplets, by either mechanism, affect the gas temperature through heat and mass transfer and, with sufficient quantities of droplets can bring the two-phase system back to near equilibrium conditions. Heterogeneous nucleation forms droplets close to the size of the initial contaminant, while for homogeneous nucleation the droplets appear at a critical radius calculated based on gas phase conditions to be:

$$r_{crit} = \frac{2\sigma T_s}{\rho_f h_{fg}\Delta T} \tag{11}$$

where T_s is the saturation temperature at local pressure, ρ_f, the density of the water, h_{fg} the equilibrium latent heat, σ liquid surface tension and ΔT is the supercooling temperature equal to $T_s(p) - T_g$.

The number of particles released into the flow as a result of homogeneous nucleation is calculated based on classical nucleation theory [13] to be:

$$J_{Hom} = \frac{q_c}{1+\eta}\left(\frac{2\sigma}{\pi m^3}\right)^{1/2}\frac{\rho_g}{\rho_f}\exp\left(-\frac{4\pi r_{crit}^2\sigma}{3KT_g}\right) \tag{12}$$

where η is defined as the following

$$\eta = \frac{\gamma-1}{\gamma+1}\frac{h_{fg}}{RT_g}\left(\frac{h_{fg}}{RT_g}-\frac{1}{2}\right) \tag{13}$$

and q_c is the condensation coefficient, K Boltzmann's constant, m the mass of one water molecule, γ specific heat ratio and R gas constant. All of equations 11 thru 13 present the generally accepted form (with only minor variations) of the classical nucleation model for wet steam in turbines, and is discussed thoroughly in reference [16].

Heterogeneous nucleation follows a similar formulation as homogeneous nucleation, with modifications for the presence of foreign nuclei and water interfacial contact conditions. In the heterogeneous nucleation model used for this study only spherical nucleation sites are considered and we do not consider water chemistry issues. For the purposes of the present study a more sophisticated nucleation model was not deemed necessary. The general form of the heterogeneous nucleation equation is then [17]:

$$J_{Het} = 4\pi R^2 n_p J_0 \exp\left(-\frac{G^*}{KT_g}\right) \tag{14}$$

where J_0 is the nucleation prefactor and is reported as $10^{25}\,cm^{-2}s^{-1}$ in many studies [17,18]. In addition n_p is the number of foreign particles per mixture mass present in the domain, R is the average radius of the particles, and G^* is the critical free energy of the cluster calculated with:

$$G^* = \frac{4\pi r_{crit}^2\sigma}{3} f(m,z) \tag{15}$$

where $f(m,z)$ is a correction factor [17] to account for contact conditions between water droplet and the foreign nuclei. The correction factor is calculated from:

$$f(m,z) = \frac{1}{2} + \frac{1}{2}\left(\frac{1-mz}{\kappa}\right)^3 + \frac{z^3}{2}\left[2 - 3\left(\frac{z-m}{\kappa}\right) + \left(\frac{z-m}{\kappa}\right)^3\right]$$
$$+ \frac{3mz^2}{2}\left(\frac{z-m}{\kappa} - 1\right) \tag{16}$$

where $m = \cos\theta$, θ is the contact angle, and z and κ are functions of the form:

$$z = \frac{R}{r_{crit}},\ \kappa = \left(1 + z^2 - 2mz\right)^{1/2} \tag{17}$$

The preceding equations describe the models for initiating phase transition and the appearance, including how many and the initial size, of a second phase into the flow.

Following phase transition models are required to describe the growth of the droplets in an initially supercooled environment. Applying an energy balance around a spherical droplet undergoing phase change results in a growth law, *G*, for the droplet. Considering the small sizes of the droplets considered in this work, thermal inertia of the droplet can be neglected leaving the balance of surface heat transfer and latent energy to give the equation:

$$(h_g - h_p)\frac{dm_p}{dt} = \alpha_p A_p (T_p - T_g) \tag{18}$$

where m_p is the mass of one droplet of water, α_p the convective heat transfer coefficient and A_p is the surface area of water droplet. The droplet temperature T_p is obtained as a function of droplet radius [19] as:

$$T_P = T_s(p) - \Delta T \frac{r_{crit}}{r} \tag{19}$$

The convective heat transfer coefficient is obtained through the Nusselt number:

$$Nu \equiv \frac{\alpha_p d_p}{k_g} = \frac{2}{1 + 3.78(1-v)\hat{l}/d_p \,\mathrm{Pr}_g} \tag{20}$$

where d_p is the diameter of water droplet, k_g the thermal conductivity of the gas and Pr_g is the Prantdl number, the factor *(1-v)* is a correction factor defined by Young [12] for improving the agreement of theoretical growth law with experimental condensation results at low pressure conditions. The variable $\hat{l}$ is the mean free path of the gas molecules and has the following definition:

$$\hat{l} = 1.5\mu_g \frac{\sqrt{RT_g}}{p} \tag{21}$$

Here μ_g is the gas dynamic viscosity. Applying Eq.20 and 21 to Eq.18 gives the final equation for the growth law:

$$G = \frac{k_g \Delta T(1 - r_{crit}/r)}{\rho_f (h_g - h_p)(r + 1.89(1-v)\hat{l}/\mathrm{Pr}_g)} \tag{22}$$

The above equation is considerably more complex than the form allowed in the MOM formulations as shown in Eq.7. However, the QMOM methodology allows Eq.22 to be directly applied with Eq.10 and highlights the advantage of the QMOM method which is not restricted to a particular form of growth law.

2.2.3. Mixture thermodynamic properties. The governing equations are formulated for mixture properties, with a mass fraction defining the extent of the liquid phase. The mass fraction can be obtained from the solution of the moments via the relation:

$$y = \frac{m_f}{m_m} = \rho_f \frac{4\pi}{3}\mu_3 \tag{23}$$

Furthermore the mean (Sauter) diameter required in transfer models, including standard deviation and skew of the distribution, can be calculated as follows:

$$\begin{aligned} d_{32} &= \frac{2\mu_3}{\mu_2} \\ \sigma &= \sum_{i=1}^{3} \left(2\left(r_i - \bar{r}\right)\right)^2 w_i \\ \gamma &= \frac{1}{\mu_0}\sum_{i=1}^{3}\left(\frac{r_i - \bar{r}}{\sigma}\right)^3 w_i \end{aligned} \tag{24}$$

Where d_{32} is the Sauter mean diameter, σ the standard deviation and γ the skewness. Phase transition as modeled in this study occurs under metastable conditions of which there is very little experimental data. Standard practice is to extrapolate equations of state (developed for superheated conditions) into the metastable region. The properties as used in this study are described in Appendix A. An important variable in the solution is the gas phase temperature, which is supercooled leading up to phase transition. Knowing the value of the mixture internal energy, e, (obtained from the total internal energy in Eq.1) the gas phase value (e_g) is obtained with:

$$e_g = \frac{e - (ye_f)}{1 - y} \tag{25}$$

from which the gas temperature is obtained. Furthermore the gas density can be obtained using:

$$\rho_g = \frac{\rho(1-y)}{1 - y\rho\rho_f^{-1}} \tag{26}$$

after which the local pressure of the mixture is calculated through the equation of state. See Appendix A for the definition of liquid internal energy e_f and the calculation of gas temperature and pressure.

3. Numerical solution

3.1. Discretization of Transport Equations

For the discretization of the mixture governing equations (Eq.1) we use a high resolution upwind Roe scheme [20,21]. The second order Lax-wendroff explicit scheme is selected for the time discretization. The predictor step determines flow conditions at an intermediate step *n+1/2:*

$$\frac{1}{\Delta t/2}\left[(SQ)^{n+1/2}-(SQ)^{n}\right]+\frac{1}{\Delta x}\left[F_E^n-F_W^n\right]-H_s^n=0 \qquad (27)$$

where the F_W^n and F_E^n are the numerical fluxes evaluated at the faces of the control volume. With the flow conditions obtained at time level n+1/2, the corrector step completes the time step to the level of *n+1* as follows

$$\frac{1}{\Delta t/2}\left[(SQ)^{n+1}-(SQ)^{n}\right]+\frac{1}{\Delta x}\left[F_E^{n+1/2}-F_W^{n+1/2}\right]-H_s^{n+1/2}=0 \qquad (28)$$

For the spatial discretization a third order upwind-biased algorithm with a MUSCL extrapolation method is used [20]. This extrapolation strategy provides the left (*L*) and right (*R*) values of the flow conditions at the cell face of each control volume. In this approach the nodal values are assumed to be known and the extrapolation provides values on both *L* and *R* sides of each cell face.

$$q_E^L=q_j+\frac{1}{4}\left[(1-\kappa)(q_j-q_{j-1})+(1+\kappa)(q_{j+1}-q_j)\right] \qquad (29)$$

$$q_E^R=q_{j+1}+\frac{1}{4}\left[(1-\kappa)(q_{j+2}-q_{j+1})+(1+\kappa)(q_{j+1}-q_j)\right]$$

In Eq.29 the subscript E denotes the east face of the control volume. $\kappa = 1/3$ corresponds to a choice of third-order upwind biased for spatial discretization and *q* denotes the flow conditions described above.

Based on the acquired *L* and *R* side fluxes and using Roe's scheme, the numerical flux at the face of a cell is obtained as

$$F_E=\frac{1}{2}\left(F_E^R+F_E^L\right)-\frac{1}{2}\sum_{k=1}^{3}\left|\hat{\lambda}_E^{(k)}\right|\delta w_E^{(k)}\hat{T}_E^{(k)} \qquad (30)$$

where λ is the eigenvalue of the Jacobian flux matrix, *T* is the related eigenvector and δw is the wave amplitude vector. The same formulation applies for the west face of the control volume. A more complete description of the implementation is provided in reference [22].

3.2. Overall Solution strategy

With all of the relevant equations now presented we can present the overall solution methodology.

At time level *n+1/2*

- Obtain hydrodynamic properties (u, ρ and e_t) at time *n+1/2* based on methodology outlined in section 3.1.
- Compute growth law (Eq.22) and nucleation (Eq.11-17) for each node using droplet sizes, r_i, and weights, w_i, of size distribution at *n*.
- Solve moment transport equations (Eq.10) with quadrature level of *n*=3 to obtain moments at new time level *n+1/2*.
- With new moments use QMOM to obtain droplet sizes, r_i, and weights, w_i, of size distribution at *n+1/2*.
- Update thermodynamic properties (Appendix A and Eq. 23-26).

Repeating the procedure for time level *n+1* to complete the time step.

4. Validation

Before exploring the application of the QMOM methodology to more complex two-phase flow conditions some initial testing was undertaken. Here the experimental data of Moore [19] for low-pressure steam flow ($p < 0.25$ *bar*) is used. The calculations are performed on nozzles A, B, C, and D as presented by Moore. In these calculations no foreign nuclei for heterogeneous nucleation are present and therefore only homogeneous nucleation is active in the phase transition process. In Fig.1 is shown the predicted pressure profiles along the four nozzles compared to experimental data from the centerline of the nozzle. The numerical results are in good agreement with experimental data across the four nozzles. In addition Fig. 2 shows comparison between calculated droplet mean radius (based on Eq.24) and the experiments. While the predicted droplet sizes show the same trends with decreasing expansion rate (nozzle A has the highest expansion rate), the absolute levels of the predictions are somewhat off. However, considering the experimental uncertainty in droplet size measurements there is good qualitative agreement.

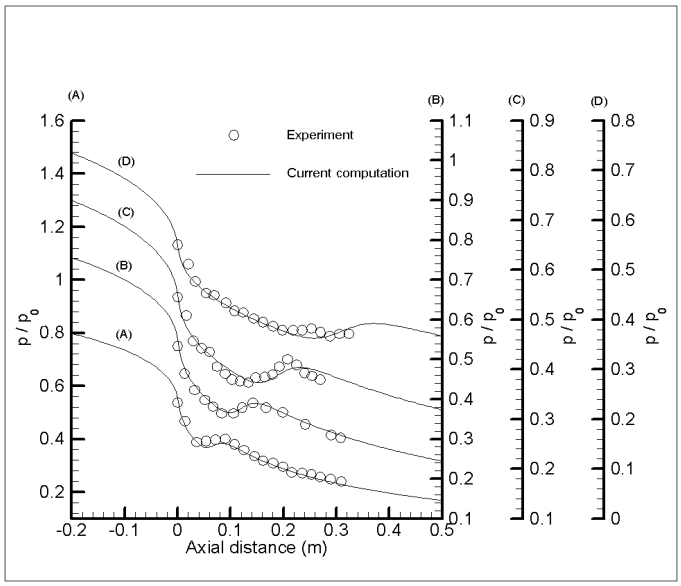

Fig.1 Comparison of pressure distribution for Nozzle (A) thru (D), p_{0in} = 25 kpa, $(T_{0in})_{A,B,C,D}$ = 354.6, 357.6, 358.6, 361.8 K

As a further verification of the model, the influence of heterogeneous nucleation on homogeneous phase transition and the resultant centerline pressure profile is examined. These results are shown in Fig. 3. The strength of heterogeneous nucleation has a dependence on concentration of nucleation sites as well as their size. As shown in Fig. 3, for sites with mean radius of $0.01\mu m$ and concentration of $N_{Het}=10^{10}kg^{-1}$ heterogeneous nucleation has little influence on flow conditions and homogeneous nucleation is dominant (as shown by the strong pressure rise). As the number of nucleation sites are

increased (holding the size the same), more droplets appear through heterogeneous phase transition and reduces the strength of the centerline pressure rise. Increasing the concentration to the level of $N_{Het} = 10^{19} kg^{-1}$ leads to the removal of the centerline pressure rise and approaches an equilibrium profile. The influence of the increase of foreign nucleation sites on nozzle flow, with homogeneous nucleation, is as expected and similar to other studies [23].

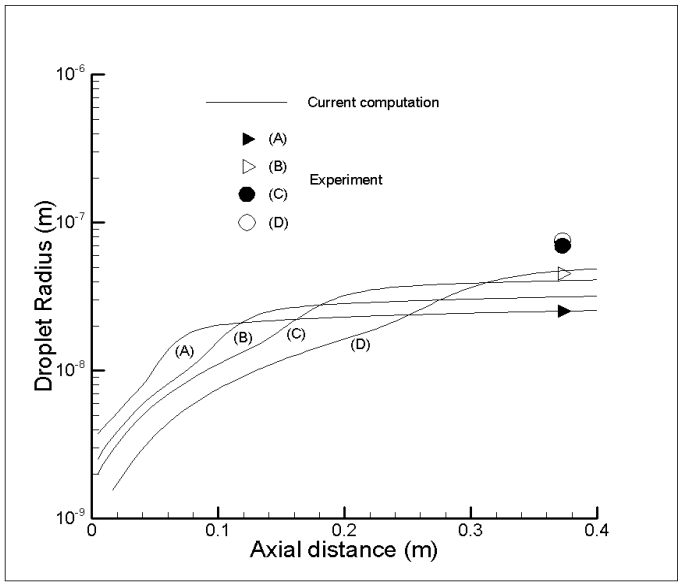

Fig.2 Comparison of droplet mean radius at a specified location for Nozzles (A) thru (D)

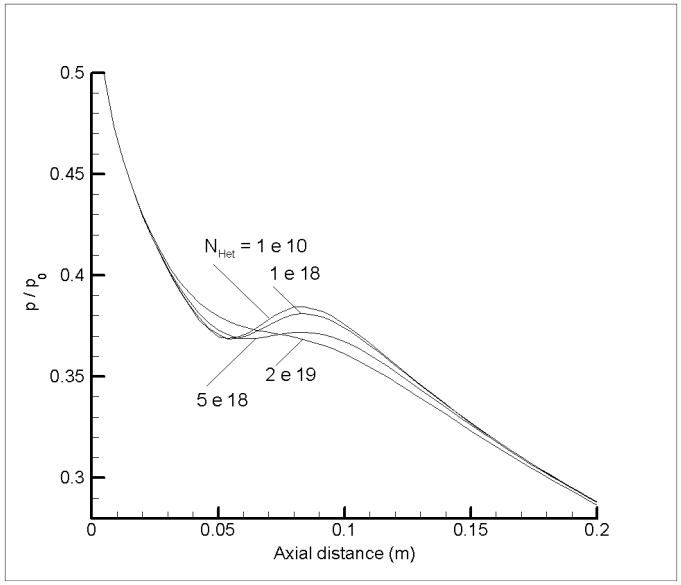

Fig.3 Relative pressure along the centerline of the nozzle for different particle concentrations, $R_{Het} = 10^{-8}$ m

5. Results and discussion

The performance of QMOM is now evaluated through tests that examine the evolution of the polydispersed droplet statistics under combinations of heterogeneous and homogeneous nucleation. Before proceeding an important clarification should be made regarding the distributions predicted by QMOM. The Gaussian quadrature that underlies QMOM does not rely on a fixed range of droplet sizes, but allows the size range (and the associated weights) to evolve with the solution. This type of quadrature is known to have a high level of accuracy in representing the integral properties of the underlying distribution [11,15]. For nonequilibrium predictions the essential quantities for accuracy are the integral surface area and volume of the distribution that impact heat and mass transfer, and subsequent transport of conserved properties. Therefore while the distributions to be presented may appear very coarse, i.e. only three sizes and weights, they preserve with high accuracy the integral quantities that appear in Eq. 10 (via summations).

The test cases are conducted using nozzle (A) of Moore. The first case has a foreign nuclei concentration of $N_{Het} = 10^8\ kg^{-1}$ with a mean radius of 0.1 μm and the results are presented in Figs.4 and 5. In Fig.4a it can be seen that with this low foreign nuclei count homogeneous nucleation dominates (as is seen in the nucleation rate inset) providing the primary contribution to the polydispersed droplet size spectrum. The evolving size distribution along the nozzle is now presented at four locations as indicated in Fig.4a with details given in Figs.4b thru e. By location one (see Fig. 4b at $x = 0.005\ m$) both nucleation processes have contributed to the sizes present, with clearly both opposing size scale present and the weight significantly skewed to the homogeneously generated droplets. At locations two through four we see the influence of the growth of small droplets in the supercooled environment as the distribution moves toward larger sizes. Note that the largest droplet sizes associated with heterogeneous nucleation are still present, but insignificant, with no representation on the scale. However the influence of the larger droplets is still present in the evaluation of the sizes and weights of the distribution, and therefore the presence of the larger droplets are maintained in evaluating the integrals of the distribution.

In Fig.5 is shown the evolution of the mean, standard deviation and skew of the distribution along the nozzle length obtained with Eq.24. The sudden appearance of the homogeneous nucleated droplets is apparent. An increase in the standard deviation of the distribution occurs as the small droplets grow in size and have more influence. The droplet skew which is initially large at the moment of homogeneous nucleation disappears as the small droplets move toward the larger sizes. The larger droplets interact with the vapor phase at a slower time scale (i.e. their growth is small) and their dynamics have little influence over the length of the nozzle.

The second test case considers a significant level of heterogeneous nucleation interacting with homogeneous nucleation. In this case the foreign particle concentration is 10^{16} kg^{-1} and the average particle size remains at the previous size of 0.1 μm. Similar to the results of the previous test case

predictions are shown in Figs.6 and 7. Increasing the number of foreign particles leads to a much higher level of heterogeneous nucleation, and consequently decreases the influence of homogeneous phase transition. This can be seen in the nucleation inset in Fig. 6a. The heterogeneous nucleation has a lower threshold for initiation of water droplets and therefore larger droplets appear earlier in the nozzle. The reduction in strength of the homogeneous nucleation removes the typical pressure rise associated with purely homogeneous phase transition.

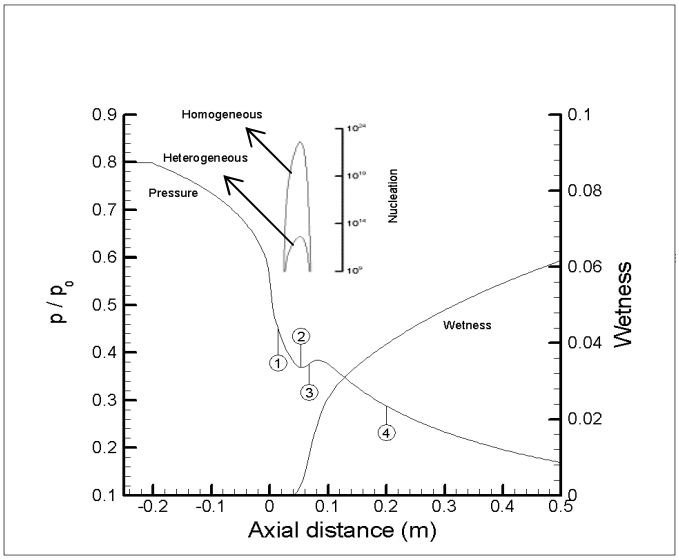

(a)

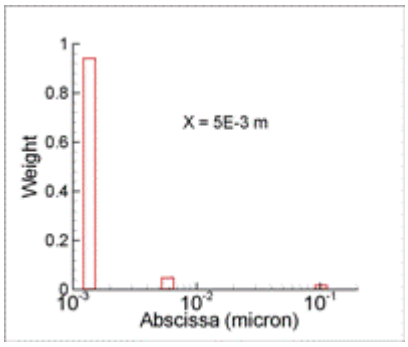

(b)

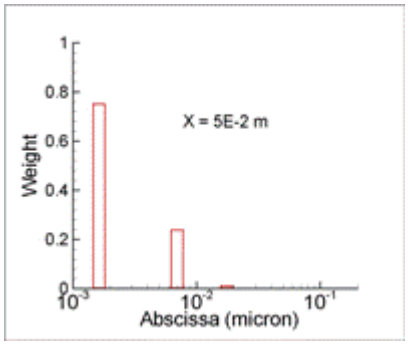

(c)

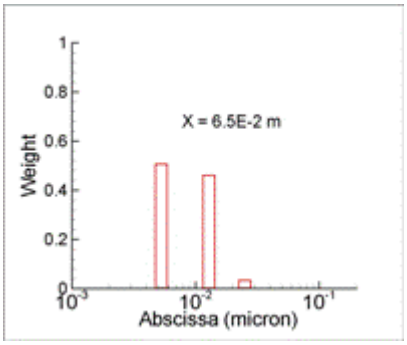

(d)

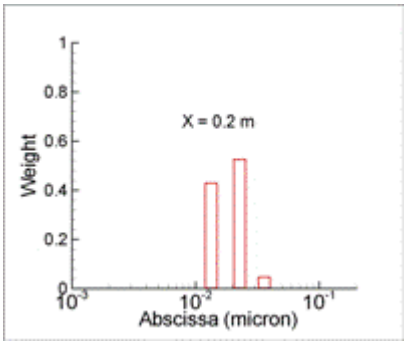

(e)

Fig. 4 (a) QMOM results for normalized pressure, wetness and nucleation, N_{Het} = 10^8 kg^{-1} and R_{Het}=0.1μm (b),(c),(d) and (e) droplet size and weight distribution at locations (1),(2),(3) and (4)

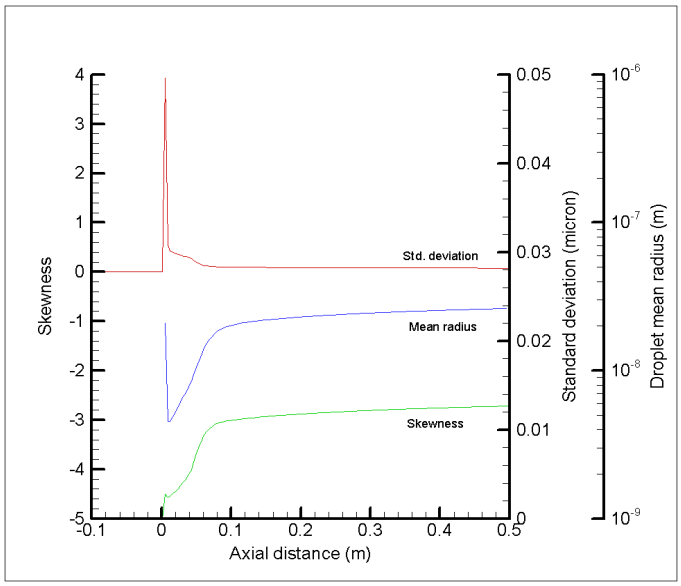

Fig. 5 Centerline value of mean droplet radius, skewness and std. deviation, N_{Het} = 10^8 kg^{-1} and R_{Het}=0.1μm

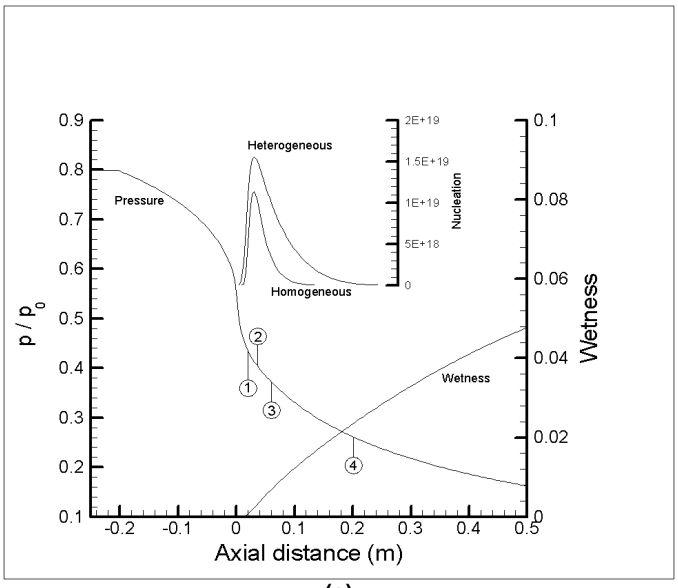

(a)

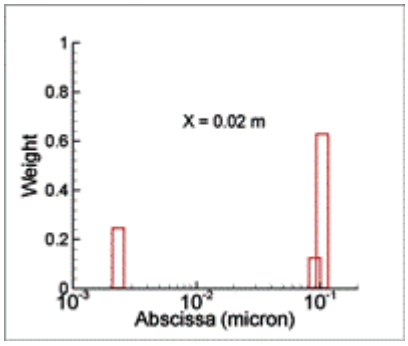

(b)

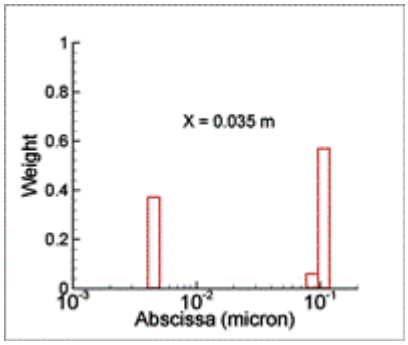

(c)

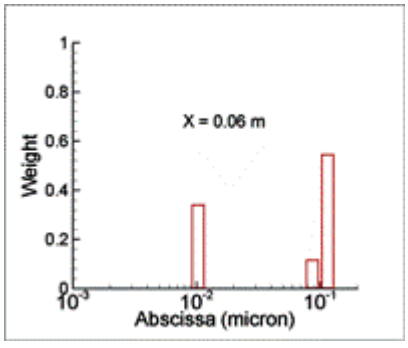

(d)

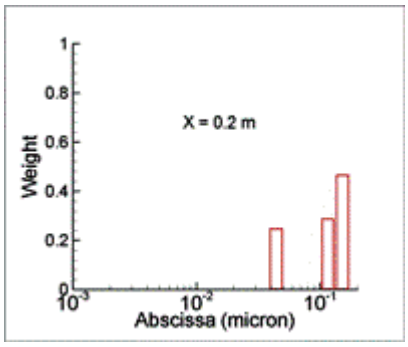

(e)

Fig.6 (a) QMOM results for normalized pressure, wetness and nucleation, N_{Het} = 10^{16} kg^{-1} and R_{Het}=0.1μm (b),(c),(d) and (e) droplet size and weight distribution at locations (1),(2),(3) and (4)

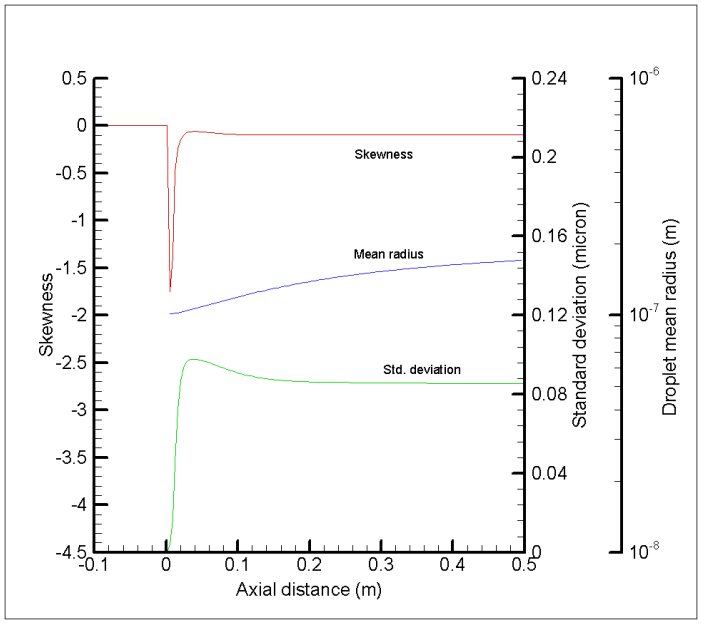

Fig.7 Centerline value of mean droplet radius, skewness and std. deviation, N_{Het} = 10^{16} kg^{-1} and R_{Het}=0.1μm

Figure 6b shows the droplet size distribution at location one which now appears quite different than in the first case (Fig. 4b). The weights have moved toward the heterogeneous droplet sizes where a slight distribution has developed according to their earlier appearance in the nozzle.

However the small droplets are more reactive in the supercooled environment and grow quickly so that the distribution narrows towards the larger size regimes (as seen in Figs.6c thru e). In the end we have a distribution straddling the 0.1 μm size range. The evolution of the statistics is shown in Fig. 7 with the mean diameter growing much more slowly, relative to the previous case, with the dominance of the larger droplet sizes. Furthermore, in comparison to case one, the resulting standard

deviation is much larger as the homogeneously nucleated droplets and heterogeneously generated ones are both present in significant quantities.

6. Conclusions

The QMOM methodology for representing polydispersed droplet distributions has been successfully applied to transonic flow conditions with phase transition. The conditions, including phase transition mechanisms, are similar to that present in low-pressure steam turbine flow.

Preliminary validation of QMOM by comparison of pressure distribution and the mean droplet size along the centerline of a supersonic nozzle indicates that the general physics of the phenomena are accurately captured. Simple verification of the heterogeneous nucleation model through its influence on nozzle centerline pressure distributions, with homogenous nucleation, also indicate physical realism. It could be concluded that for the present study, the statistics of the polydispersed droplet could be accurately examined, and two droplet formation scenarios were subsequently chosen. The two cases considered the droplet distributions present with strong homogeneous/weak heterogeneous and moderate homogeneous/strong heterogeneous phase transitions. Results indicate that the QMOM predicts physically realistic statistics for the evolving distribution along the length of the nozzle.

The numerical tests conducted indicate that the QMOM methodology may provide a viable CFD modeling approach for handling polydispersed steam flow as present in the low pressure stages of a steam turbine. However the present study only examines distributions where droplets are transported at the gas phase velocity. In real flows larger droplets tend to move at their own velocity which this study does not consider. Generally such droplets would be larger than the droplet sizes considered in this study. Finally, the methodology should also be considered for cases where shock structures are present to test the QMOM methodology in cases where strong property discontinuities are present. Preliminary studies by the authors indicate that the methodology is robust but a thorough study needs to be undertaken before final conclusions can be drawn.

7. Acknowledgements

The authors would like to acknowledge the support of the Natural Sciences and Engineering Research Council of Canada under an on-going Discovery Grant.

References

[1] Bakhtar, F., Mahpeykar, M.R. and Abbas, K.K., (1995) “An Investigation of Nucleating Flows of Steam in a Cascade of Turbine Blading-Theoretical Treatment”, Transaction of the ASME: Journal of Fluids Engineering, vol. 117, pp. 138-144.

[2] Young, J.B., (1992) “Two-Dimensional, Nonequilibrium, Wet Steam Calculations for Nozzles and Turbine Cascades”, Trans. ASME.: J. Turbomachinery, vol. 114, pp. 569-579.

[3] White, A.J. and Young, J.B., (1993) “Time-Marching Method for the Prediction of Two-Dimensional, Unsteady Flows of Condensing Steam”, Journal of Propulsion and Power, vol. 9, no. 4, pp. 579-587.

[4] McCallum, M. and Hunt, R., (1999) “The Flow of Wet Steam in a One-Dimensional Nozzle”, Int. J. Numer. Meth. Engng., vol. 44, pp. 1807-1821.

[5] Gerber, A.G., (2002) "Two-Phase Lagrangian/Eulerian Model for Nucleating Steam Flow", Journal of Fluids Engineering, Vol. 124, No. 2, pp. 465-475.

[6] Gerber, A.G., Kermani, M.J., (2004) “A Pressure Based Eulerian-Eulerian Multiphase Model for Condensation in Transonic Steam Flows”, Int. Journal of Heat and Mass Transfer, Vol. 47, pp. 2217-2231.

[7] Winkler, G. and Schnerr, G.H., (2001) “Nucleating Unsteady Flows in Low-Pressure Steam Turbine Stages”, Proc. Instn Mech Engrs Part A, vol. 215, pp. 773-781.

[8] Bohn, D.E., Surken, N., and Kreitmeier, (2003) “Nucleation phenomena in a multi-stage low pressure steam turbine”, Proc. Instn Mech. Engrs: J. Power and Energy, Vol. 217, pp. 453-460.

[9] Hulburt, H. M., and Katz, S., (1964) “Some problems in particle technology” Chem. Eng. Sci., Vol.19, p.555

[10] McGraw, R., (1997) ”Description of Aerosol Dynamics by the Quadrature Method of Moments”Aerosol Sci. Tech., 27, 255

[11] Gerber, A., Mousavi, A., (2006) “Application of Quadrature method of moments to the polydispersed droplet spectrum in transonic steam flows with primary and secondary nucleation” J. Appl. Math. Modeling, Accepted for publication, March 2006

[12] White,A.J, and Hounslow.M.J., (2000) “Modelling droplet size distribution in polydispersed wet-steam flows”Int.J.Heat and mass transfer, Vol.43, p.1873

[13] McDonald, J.E. 1962-3, "Homogeneous Nucleation of Water Vapor Condensation. I. Thermodynamic Aspects", Am. J. Physics, Vol. 30, pp. 870 - 877.

[14] Hoffmann, K.A. , Chiang, S.T., (1993) “ Computational fluid dynamics for engineers” Vol.2, Engineering education system, Wichita, Kansas.

[15] Marchisio, D. L., Fox, O., and Vigil, R.D., (2003) “Quadrature Method of Moments for Population-Balance Equation” AIchE J., 49, 1266

[16] F. Bakhtar, J.B. Young, A.J. White, D.A. Simpson, "Classical nucleation theory and its application to condensing steam flow calculations", IMechE Part C:J. Mechanical Engineering Science, 2005, Vol. 219, pp.1315-1333.

[17] Lee, T.D., (1998) “Surface characterization by Heterogeneous nucleation from the vapor” PhD thesis, Harvard University.

[18] Lee, Y.L., Chou, W.S., Chen, L.H., (1998) “The adsorption and nucleation of water vapor on an insoluble spherical solid particle” Journal of Surface science, 414, pp. 363-373.

[19] Moore, M.J. and Sieverding, C.H., (1976) “Two-Phase Steam Flow in Turbines and Separators”, Hemisphere Publishing.

[20] Hirsch, C., (1990) ”Numerical computation of internal and external flows” John Wiley & Sons, Vol.2.

[21] Anderson, D.A., Tannehill, J.C., Pletcher, R.H., (1997) ”Computational fluid mechanics and heat transfer”

[22] Kermani, M. J., Gerber, A. G. and Stokie, J. M., (2006) “An application of Roe high resolution scheme to transonic two-phase flows through nozzle” Iranian journal of mechanical engineers : Transactions of the ISME (Accepted)

[23] Stastny, M., Sejna, M., (2005) “The effect of expansion rate on the steam flow with hetero-homogeneous condensation

in nozzles " Proc.IMechE Vol.219, Part A: J. Power and energy, PP. 491-497
[24] Lanczos, C., (1965)"Applied analysis" Dover, New York, p.396.
[25] White,A.J, (2003)"A comparison of modeling methods for polydispersed wet-steam flow",Int. J. Numer. Meth. Engng, Vol.57, p.819

Appendix A: Properties

The properties used in the simulations are obtained as follows. The gas phase density is obtained based on the following equation of state:

$$\rho_g = \frac{p}{RT_g} \tag{A1}$$

Assuming constant specific heat capacity (c_{vg}), the supercooling temperature, T_g , is calculated as a function of gas energy using:

$$T_g = e_g / C_{vg} \tag{A2}$$

The internal energy of the liquid is obtained through the following equation as a function of temperature.

$$e_f = E_2(T_p - 273)^2 + E_1(T_p - 273) + E_0 \tag{A3}$$

$E_0 = 2.372678E+6$
$E_1 = -2.661665E+3$
$E_2 = -1.964125$

Saturation temperature as a function of local pressure is computed as below which is suitable for low pressure steam:

$$T_S = ap^b \tag{A4}$$

where $a = 366.8223$ and $b = 0.05904$.

Gas phase properties and bulk liquid surface tension were obtained using the linear equation:

$$X = aT + b \tag{A5}$$

with the coefficients given in Table A-1.

X	a	b
$k_g(W/mK)$	6.2167×10^{-5}	1.1618×10^{-3}
Pr_g	1.6717×10^{-3}	0.3566
$\sigma(N/m)$	-1.6539×10^{-4}	0.121
$c_{pg}(J/kgK)$	0	1880
$h_{fg}(J/kg)$	-2.3998×10^{3}	3157.43×10^{3}

Table A-1. Coefficients for properties evaluated with Eq.A5